

1994031780

442523

N94-26283

**Performance Measures from the Explorer
Platform Berthing Experiment**

**Stephen Leake
NASA Goddard Space Flight Center
Greenbelt, Maryland**

Performance measures
from the
Explorer Platform berthing experiment

Stephen Leake
NASA Goddard Space Flight Center
Robotics Lab
February 17, 1993

1 Introduction

The Explorer Platform is a Modular Mission Spacecraft; it has several sub-units that are designed to be replaced on orbit. The Goddard Space Flight Center Robotics Lab undertook an experiment to evaluate various robotic approaches to replacing one of the units; a large (approximately 1 meter by 1 meter by 0.5 meter) power box. The hardware (see figure 1) consists of a Robotics Research Corporation K-1607 (RRC) manipulator mounted on a large gantry robot, a Kraft handcontroller for teleoperation of the RRC, a Lightweight Servicing Tool (LST) mounted on the RRC, and an Explorer Platform mockup (EP) with a removable box (MMS) that has fixtures that mate with the LST. Sensors include a wrist wrench sensor on the RRC, and Capaciflectors [Vranish91] mounted on the LST and the MMS. There are also several cameras, but no machine vision is used. The control system for the RRC is entirely written by Goddard [Leake91]; it consists of Ada code on three Multibus I 386/387 CPU boards doing the real-time robot control, and C on a 386 PC processing Capaciflector data. The gantry is not moved during this experiment.

The task is the exchange of the MMS; it is removed and replaced. This involves four basic steps: mating the LST to the MMS, demating the MMS from the EP, mating the MMS to the EP, demating the LST from the MMS. Each of the mating steps must be preceded by an alignment to bring the mechanical fixtures within their capture range.

Two basic approaches to alignment are explored; teleoperation with the operator viewing thru cameras, and Capaciflector based autonomy. To eval-

2 ALIGNMENT

uate the two alignment approaches, we ran several runs with each approach, and recorded the final pose. Comparing this to the ideal alignment pose gives accuracy and repeatability data. In addition, the wrenches exerted during the mating tasks were recorded; this gives information on how the alignment step affects the mating step.

There are also two approaches to mating; teleoperation, and impedance-based autonomy. The wrench data taken during mating using these two approaches is used to evaluate them.

Section 2 describes the alignment results, Section 3 describes the mating results, and finally Section 4 gives some conclusions.

2 Alignment

The two alignment tasks are aligning the LST for mating with the MMS, and aligning the MMS for mating with the EP. Two methods were used for each task; teleoperation, and Capaciflector-based autonomy.

For teleoperation, we used the Langley rate control algorithm. One experienced operator performed all the runs. The Kraft hand-controller acts like a 6 DOF joystick; the rate of the RRC tool frame is proportional to the displacement of the Kraft from a reference frame. In a traditional joystick, there is a centering spring force returning the joystick to the reference frame; in the Langley algorithm, this centering force has a constant magnitude, not proportional to the displacement. This allows wrench feedback to be added to the centering force without operator confusion. On the RRC, there is a Cartesian impedance algorithm using the wrench sensor, that makes the RRC tool frame behave like a pure damper; it relaxes when any force is applied. Thus if the tool is against a surface, and the operator pushes the hand-controller into the surface, the hand-controller commands a constant rate, which is turned into a constant force by the damper algorithm on the RRC. At the same time, the wrench sensed by the RRC wrench sensor is fed back to the motors on the hand-controller. Wrench feedback ratios of 1:1 can be achieved with this algorithm. Since the alignment task is primarily free-space positioning, the wrench feedback was low for this task, to mask noise and errors in the gravity model of the loads carried by the wrench sensor. Three cameras were used during teleop; one on the LST (only used

2 ALIGNMENT

for mating the LST to the MMS), one giving an overall view of the RRC and EP, and one giving a good view of the MMS mounted on the EP.

For Capaciflector-based autonomy, there are two Capaciflectors mounted on the LST, and six on the MMS. Alignment is a 6 DOF task; this is easily accomplished with the six sensors on the MMS. For the LST, there is no way to place six sensors to get a full alignment. So a sequential approach is used; first the two sensors are leveled against a surface, then they find an edge, then they find a bump along the edge, etc. Each step in the sequence can find two degrees of freedom; we used a 7 step sequence to help eliminate errors.

For each task, a "perfect" goal pose was defined manually (using rulers and direct vision to align the LST and MMS). Then 10 runs for each combination of task and approach were made, recording the final pose for each run. The accuracy is defined as the mean error between the "perfect" goal pose and the 10 actual poses; the repeatability is the standard deviation of the same error. For the MMS, there are not enough visual cues to allow the operator to align the MMS with the EP without contact. So the MMS_TELEOP task did both alignment and initial contact; the MMS_CAPACIFLECTOR task did not contact. The following table summarizes the results, and the scatter plots in figures 2 thru 5 show the raw data.

run	time (sec)	translation (mm)		rotation (radians)	
		accuracy	repeat	accuracy	repeat
LST_TELEOP	53 +- 10	7.39	5.29	0.02789	0.07483
LST_CAPACIFLECTOR	123 +- 0.5	5.69	0.45	0.01883	0.00096
MMS_TELEOP	42 +- 10	7.49	15.5	0.01920	0.04911
MMS_CAPACIFLECTOR	61 +- 20	2.88	11.7	0.01092	0.03554

For both tasks, teleoperation is significantly faster. The LST task shows a 23% improvement in translation accuracy from teleop to Capaciflector, and a 32% improvement in rotation accuracy. The repeatability is significantly better with the Capaciflector; a factor of 11 for translation, 77 for rotation. For the MMS task, the accuracy shows a 61% improvement in translation, and 43% improvement in rotation. The repeatability shows a 24% improvement in translation, and 27% in rotation. Remember that the teleoperation MMS task used contact for the final alignment, while the Capaciflector made no contact; the Capaciflector algorithm is more repeatable than the mechanical contact!

3 MATING

For the MMS, it often took 1 or 2 incorrect contacts before the final correct contact was made.

For the LST, the operator felt teleoperation was more reliable, while for the MMS, he felt the Capaciflector was more reliable.

3 Mating

Wrench data was logged for both LST and MMS mating, recording data from just before contact until after full contact. The fixtures in both tasks guarantee 6 DOF alignment. The LST is essentially rigid; the contact between the LST and the MMS fixture is basically a narrow cone, with a plate and two posts at the top for roll alignment. The clearance between the LST and the mating fixtures on the MMS is about 2 mm and 0.1 radians. The contact between the MMS and the EP is at three points (before the screw is fastened); there is no clearance, but the contacts are actually spherical, so some misalignment is possible. No screws were tightened or latches fastened, to simplify data analysis. Two methods were used for each mating task; Cartesian impedance control, and teleoperation. The LST mating was then repeated using a more complex impedance control. For teleoperation, one experienced operator performed all the runs, starting from the same starting point as the teleop alignment task. For autonomy, the start pose was representative of the final alignment pose using Capaciflectors. Thus the differences include differences in starting alignment as well as mating algorithm.

For teleoperation, we again use the Langley rate algorithm. The wrench feedback and RRC damper gains are adjusted to give the best operator feel, while maintaining stability. The best operator feel is achieved when the joint stiffness is very low. If the joint stiffness is high, the Cartesian impedance loop has to work very hard to overcome it, and this shows up as instability at high wrench feedback gains. However, to use a low joint stiffness, we must use gravity compensation torque, to keep the arm from sagging. Unfortunately, a design flaw in the RRC analog servo hardware prevents us from using a torque command when carrying the MMS payload, so we had to use relatively high joint stiffness for the MMS. We repeated the LST runs using a softer joint servo with gravity compensation. The actual

3 MATING

gains for each run are given in the appendix.

The performance measures are the time from first contact to stable contact, rms wrench error, and the maximum wrench. The Z axis is the mating direction; wrench error in this direction is measured only after stable contact. The following table summarizes the results; figures 6 thru 13 show the raw wrench logs for a representative run.

run	time	rms wrench error						max wrench	
		TX	TY	TZ	RX	RY	RZ	tran	rot
LST_MATE_TELEOP	14.6	1.07	3.34	14.60	0.95	0.40	0.12	53.6	2.48
LST_MATE_AUTO	6.0	1.58	1.58	22.97	1.65	3.76	0.14	79.4	8.29
MMS_MATE_TELEOP	32.2	11.3	30.7	55.6	4.69	8.07	2.36	250.3	27.8
MMS_MATE_AUTO	2.2	3.82	2.38	0.71	0.83	1.77	0.39	82.1	4.65
LST_MATE_SOFT_TELEOP	7.2	4.49	1.88	6.14	0.67	1.26	0.52	51.6	4.19
LST_MATE_SOFT_AUTO	4.5	4.60	5.01	15.7	0.82	1.77	0.27	105.4	8.11

For both tasks, teleop was slower than autonomy.

For the LST task, teleop gave lower wrench errors, and lower maximum wrenches. This is attributed to the fact that the operator used vision to refine the alignment as mating proceeded.

For the MMS task, there is a factor of at least 5 improvement in wrench errors for autonomy; the off-insertion-axis portion can be attributed to the more accurate and reliable Capaciflector alignment, while the on-insertion-axis portion is due to the more stable mating algorithm.

Note that the LST_MATE run was slightly unstable when fully mated, and that MMS_MATE_TELEOP typically made contact twice incorrectly before finally seating.

The operator would always prefer to use the autonomous impedance algorithm, not teleop. The control system is actually more complex for teleop.

The more complex gravity compensation control system gave faster times and lower on-insertion-axis forces, but higher off-insertion-axis wrench errors. It was more stable than the non-gravity compensation system.

4 CONCLUSIONS

4 Conclusions

For both tasks, the Capaciflector gave an improvement of at least 25% in alignment accuracy and repeatability. For the LST task, the repeatability improved by a factor of at least 11.

For the LST task, teleoperation alignment followed by teleoperation mating gave lower wrench errors, by a factor of about 2. For the MMS task, Capaciflector alignment followed by autonomous mating gave lower wrench errors by a factor of at least 5. These results are not conclusive; more work needs to be done to distinguish between the effects of initial alignment and mating algorithm.

We anticipate significant reductions in the wrench errors and maximum wrenches with future control system improvements, for both autonomy and teleoperation.

5 Acknowledgments

Ed Cheung of the Goddard Robotics Lab wrote the C code for the Capaciflectors, and developed the Capaciflector alignment algorithms.

6 References

[Vranish91] J. Vranish, R. McConnell, S. Mahalingam, "Capaciflector Collision-Avoidance Sensors for Robots", *International Journal of Computer and Electrical Engineering*, Vol 17 #3, 1991

[Leake91] Stephen Leake, "A Cartesian Force Reflecting Teleoperation System", *International Journal of Computer and Electrical Engineering*, Vol 17, no 3, 1991.

7 APPENDIX

7 appendix

LST_MATE_TELEOP uses teleoperation in the Langley mode, with the following parameters:

```
Motion_Scale => (others => 0.1),
Wrench_Feedback => (Active => TRUE, Scale => (others => 0.25)),
Joint_Servo =>
  (Joint_Servo_Label => ANALOG_DAMPING_NOGRAV,
   Pos_Error_Action => CLIP,
   ADN_Vel_Gain => (6.0, 6.0, 6.0, 6.0, 6.0, 4.0, 4.0)),
Cart_Impedance => (Active => TRUE,
  Bias => (others => 0.0),
  Spring => (others => 0.0),
  Damper => (1000.0, 1000.0, 1000.0, 200.0, 200.0, 100.0))
```

LST_MATE_AUTO uses Cartesian impedance control, with the following parameters:

```
Joint_Servo =>
  (Joint_Servo_Label => ANALOG_DAMPING_NOGRAV,
   Pos_Error_Action => CLIP,
   ADN_Vel_Gain => (6.0, 6.0, 6.0, 6.0, 6.0, 4.0, 4.0)),
Cart_Impedance => (Active => TRUE,
  Bias => (TZ => 40.0, others => 0.0),
  Spring => (others => 0.0),
  Damper => (4000.0, 4000.0, 4000.0, 1600.0, 1600.0, 400.0))
```

MMS_MATE_TELEOP uses teleoperation in the Langley mode, with the following parameters:

```
Motion_Scale => (others => 0.05),
Wrench_Feedback => (Active => TRUE, Scale => (others => 0.125)),
Joint_Servo =>
  (Joint_Servo_Label => ANALOG_DAMPING_NOGRAV,
   Pos_Error_Action => CLIP,
   ADN_Vel_Gain => (6.0, 6.0, 6.0, 6.0, 6.0, 4.0, 4.0)),
```


7 APPENDIX

```
Cart_Impedance => (Active => TRUE,  
  Bias => (others => 0.0),  
  Spring => (others => 0.0),  
  Damper => (4000.0, 4000.0, 4000.0, 800.0, 800.0, 800.0)),
```

MMS_MATE_AUTO uses Cartesian impedance control, with the following parameters:

```
Joint_Servo =>  
  (Joint_Servo_Label => ANALOG_DAMPING_NOGRAV.  
  Pos_Error_Action => CLIP,  
  ADN_Vel_Gain => (6.0, 6.0, 6.0, 6.0, 6.0, 4.0, 4.0)),  
Cart_Impedance => (Active => TRUE,  
  Bias => (TZ => 80.0, others => 0.0),  
  Spring => (others => 0.0),  
  Damper => (4000.0, 4000.0, 4000.0, 1600.0, 1600.0, 1600.0))
```

LST_MATE_SOFT_TELEOP uses teleoperation in the Langley mode, with the following parameters:

```
Motion_Scale => (others => 0.2),  
Wrench_Feedback => (Active => TRUE, Scale => (others => 0.5)),  
Joint_Servo =>  
  (Joint_Servo_Label => PD_GRAV.  
  Pos_Error_Action => CLIP,  
  PDG_Stiffness => (9000.0, 3562.55, 2625.63, 2341.13, 341.75, 385.42, 80.  
  PDG_Damping => (900.0, 580.59, 318.80, 281.04, 33.40, 37.04, 1.  
Cart_Impedance => (Active => TRUE,  
  Bias => (others => 0.0),  
  Spring => (others => 0.0),  
  Damper => (1000.0, 1000.0, 1000.0, 100.0, 100.0, 100.0)),
```

LST_MATE_SOFT_AUTO uses Cartesian impedance control, with the following parameters:

```
Joint_Servo =>  
  (Joint_Servo_Label => PD_GRAV,
```

7 APPENDIX

```
Pos_Error_Action => CLIP,  
PDG_Stiffness => (9000.0, 3562.55, 2625.63, 2341.13, 341.75, 385.42, 80.  
PDG_Damping => (900.0, 580.59, 318.80, 281.04, 33.40, 37.04, 1.  
Cart_Impedance => (Active => TRUE,  
Bias => (TZ => 40.0, others => 0.0),  
Spring => (others => 0.0),  
Damper => (1000.0, 1000.0, 1000.0, 100.0, 100.0, 100.0)).
```

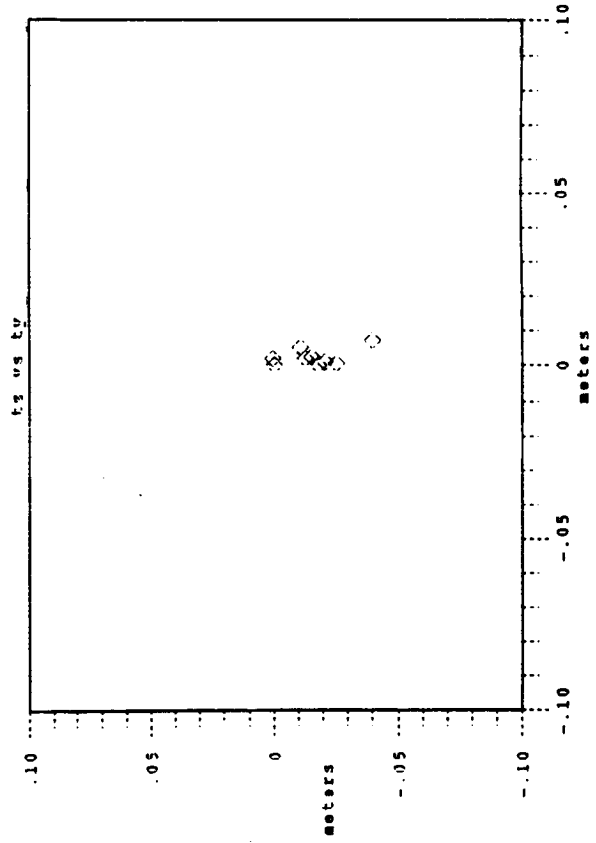
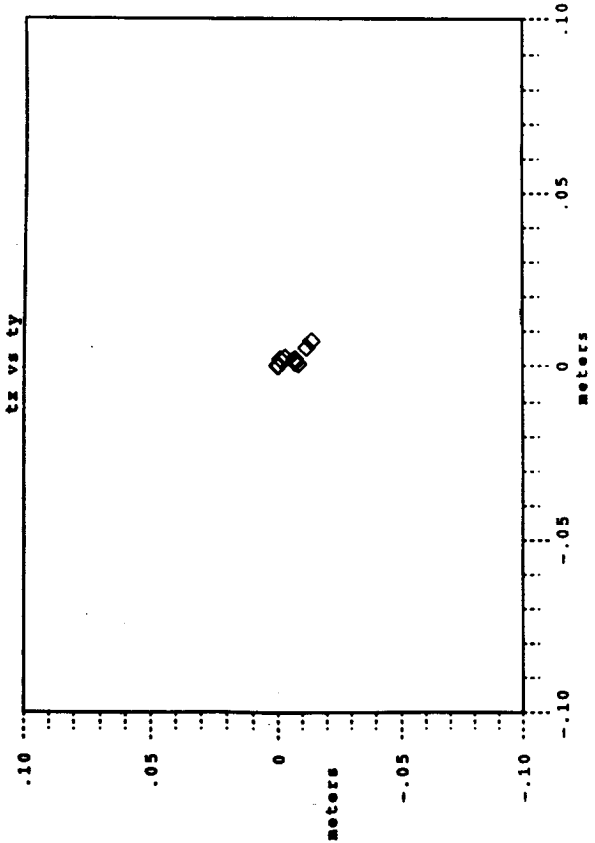
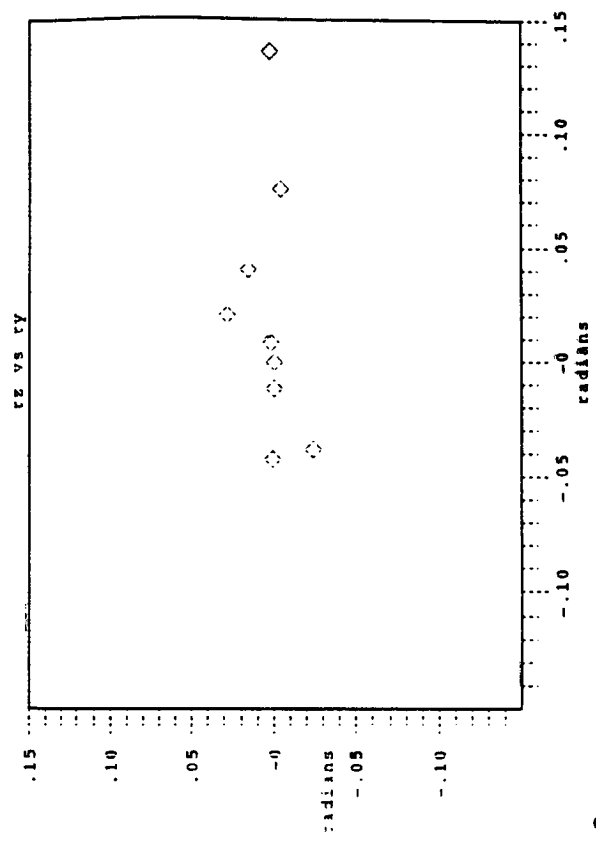
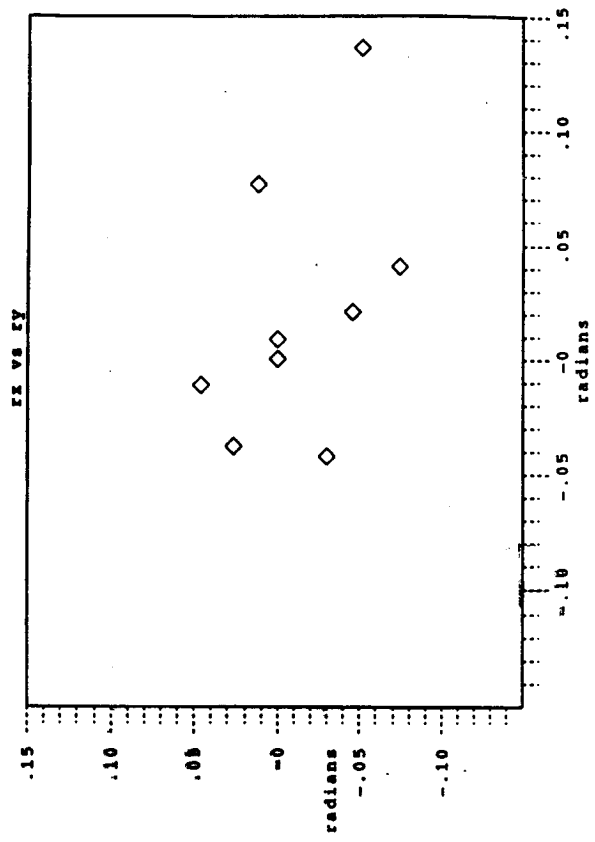


Figure 2

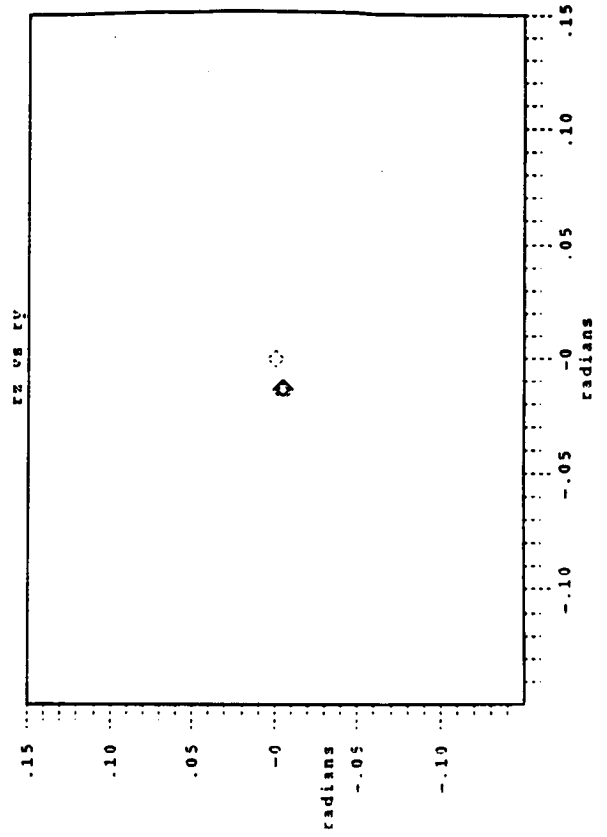
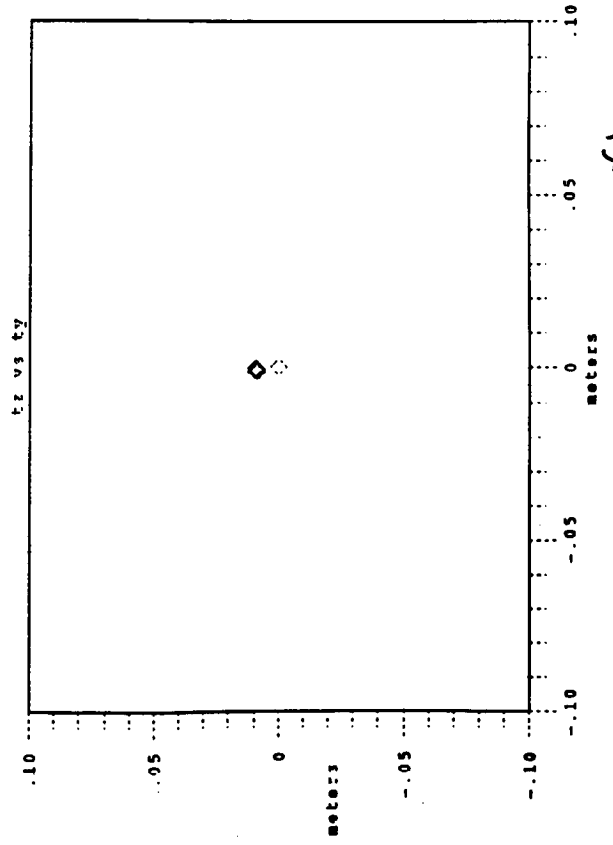
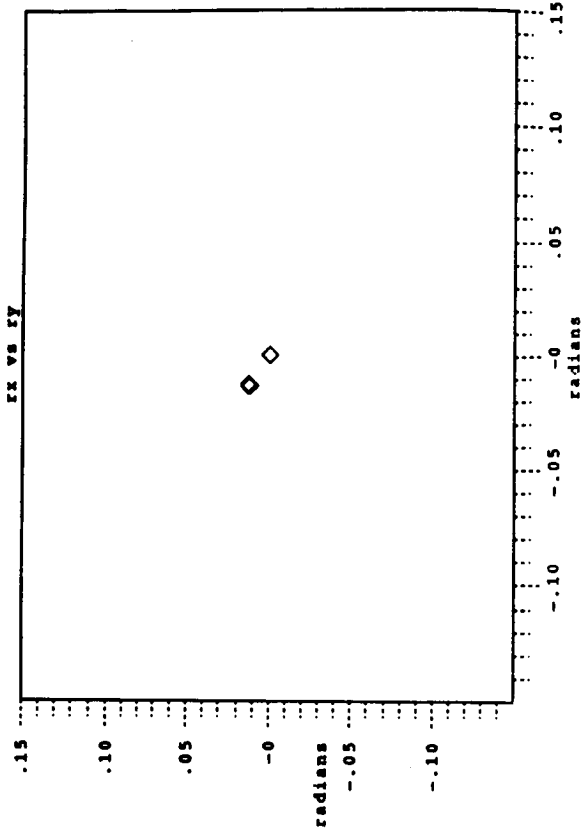
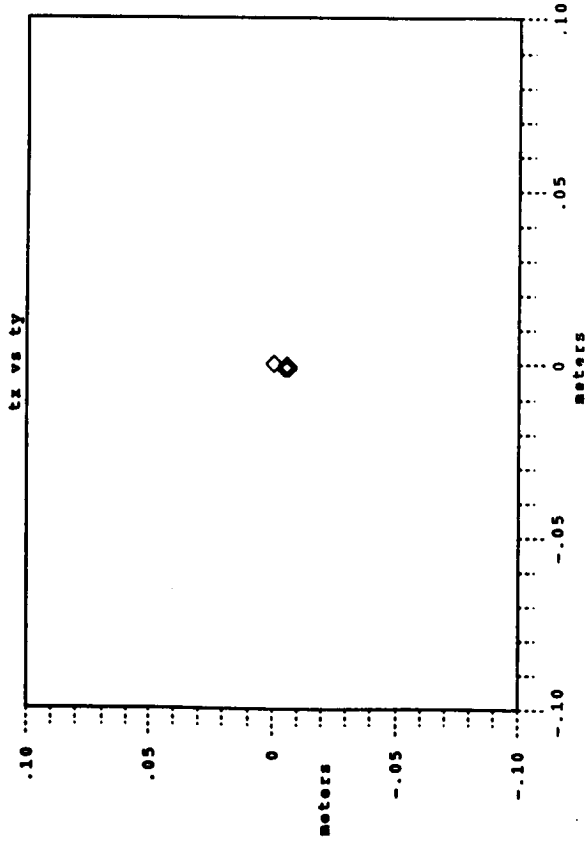


Figure 3

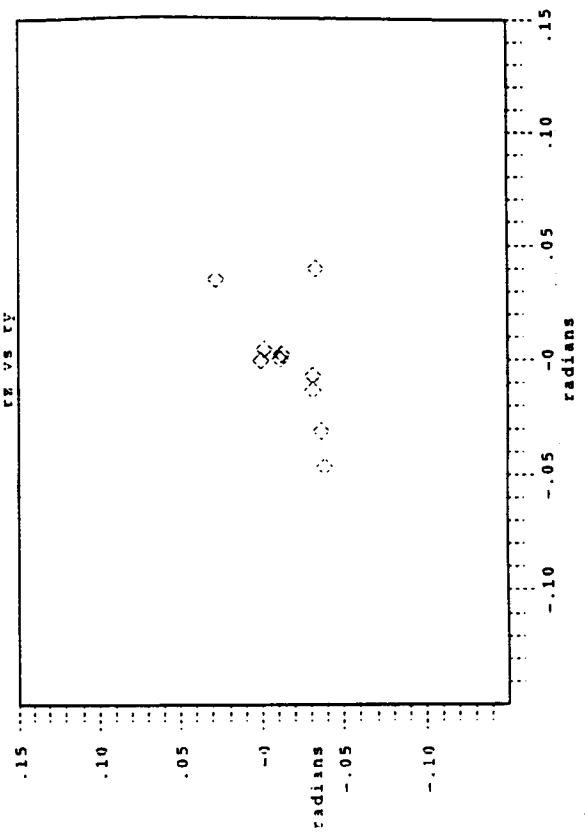
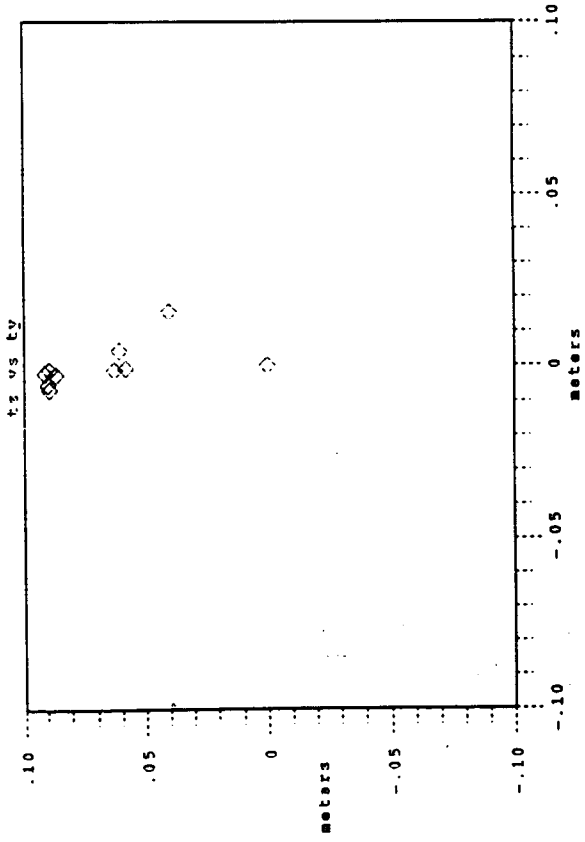
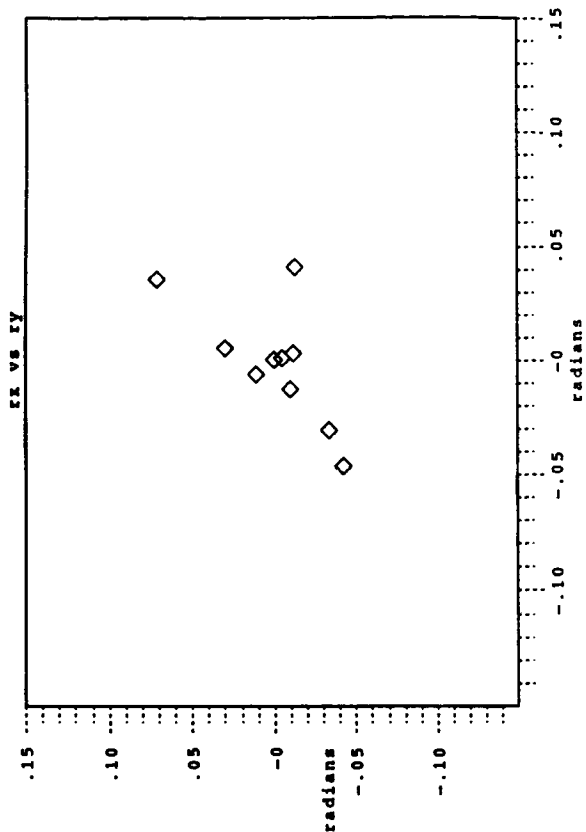
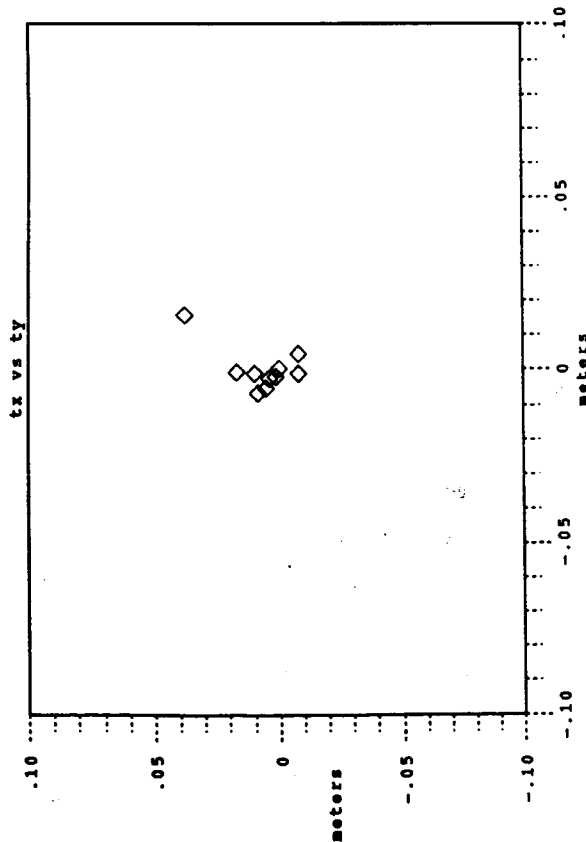


figure 4

File: EP_MMS_CAPACIFLECTOR.PLOT

Time: 14:13:46.43 17-FEB-1993

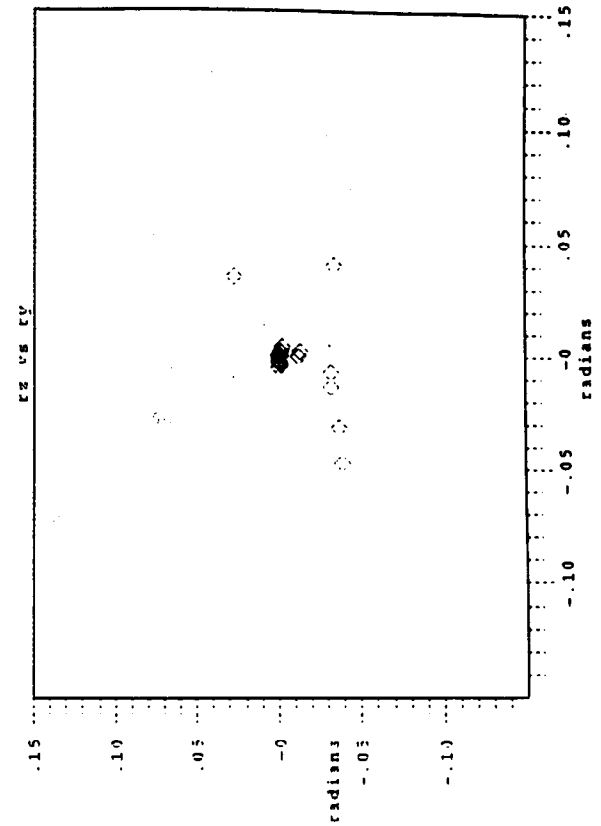
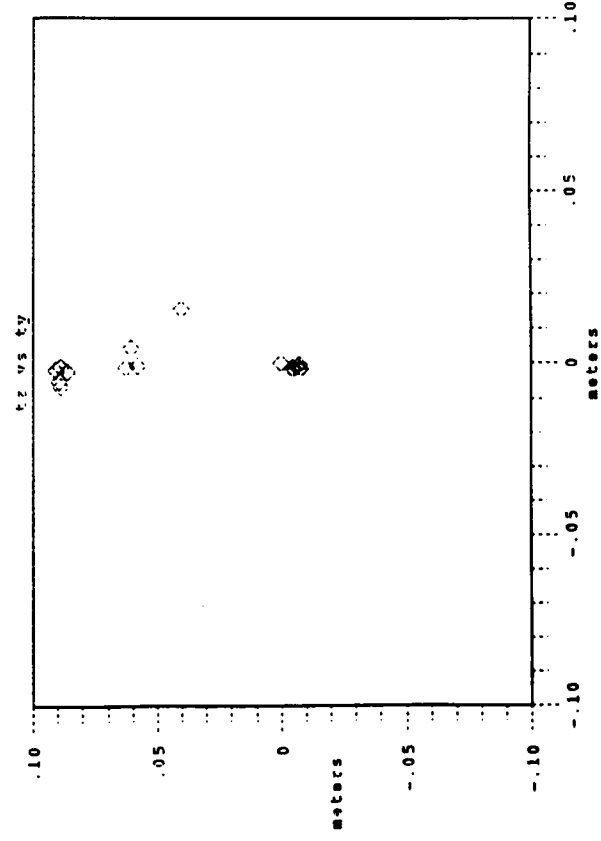
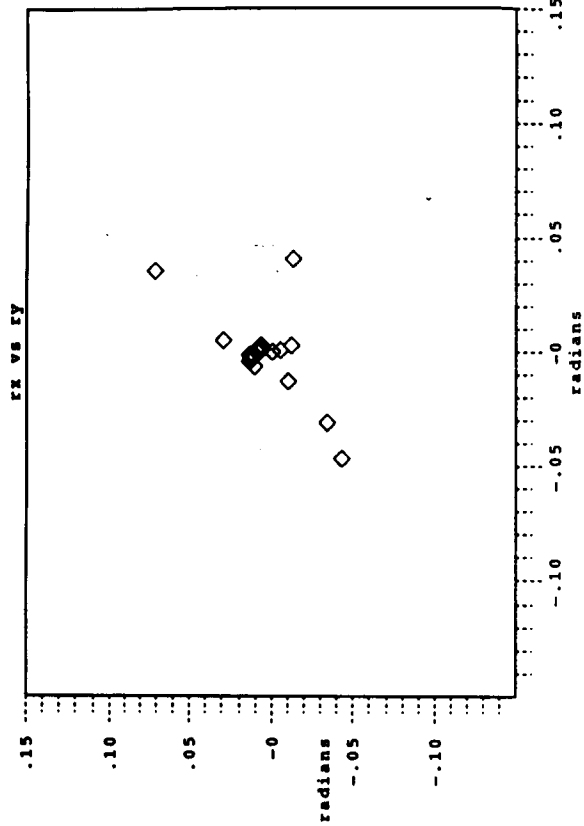
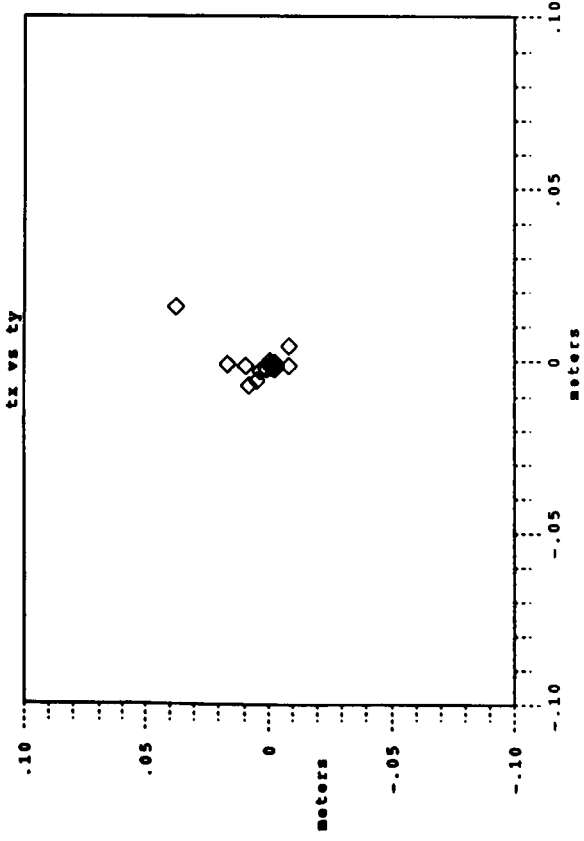


Figure 5

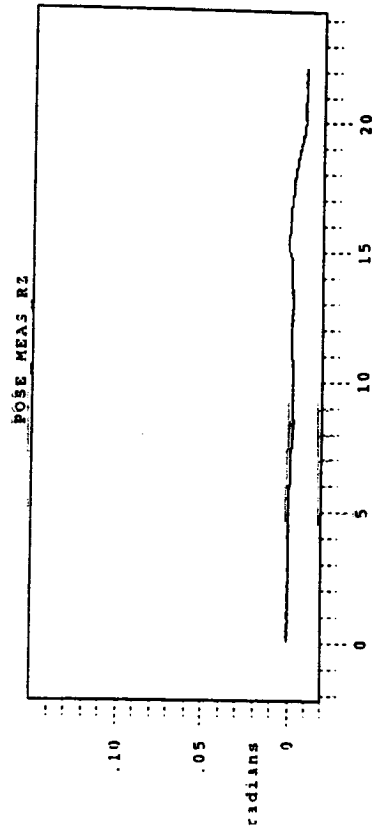
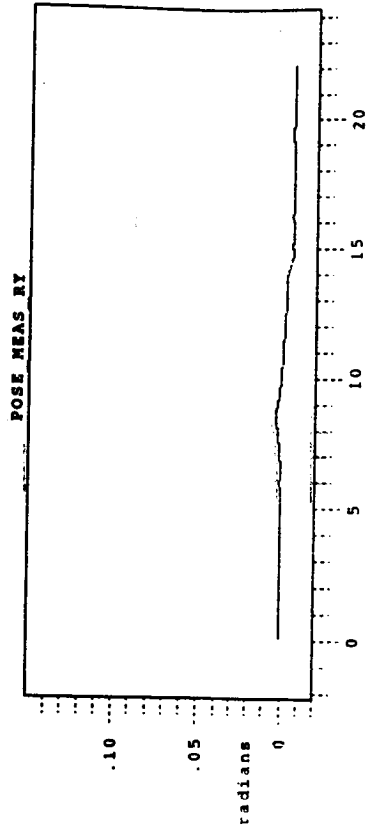
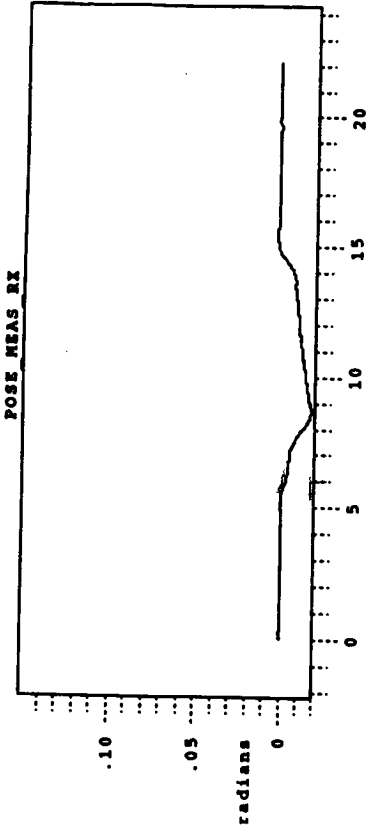
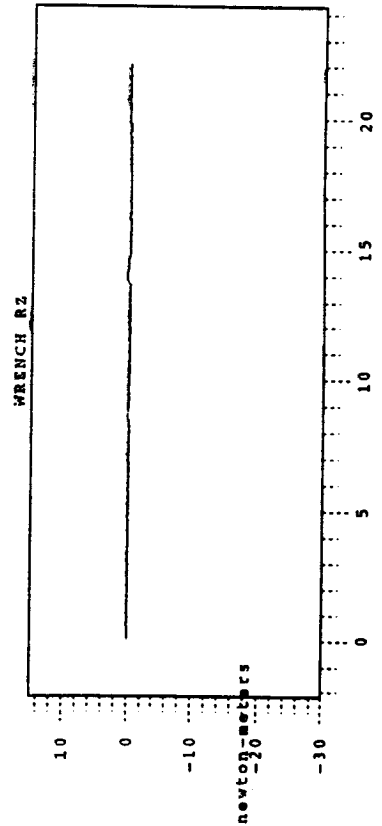
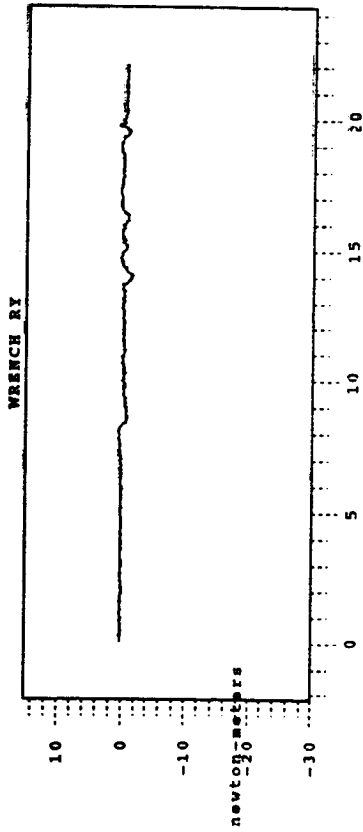
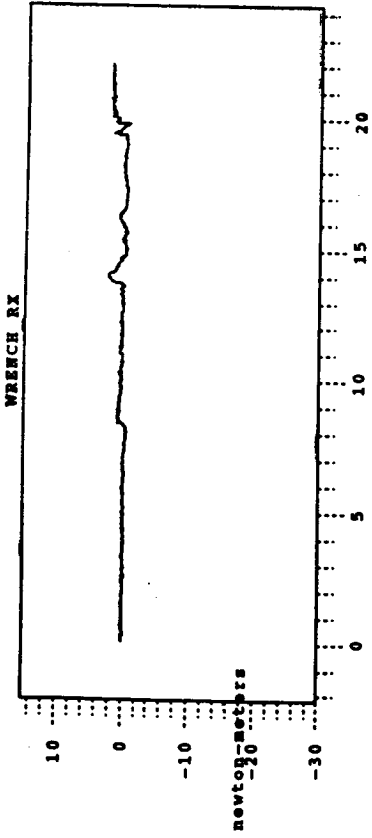


Figure 6

File: (.LSTIMATE_TELSEP.PLOT

Time: 15:39:03.36 17-FEB-1993

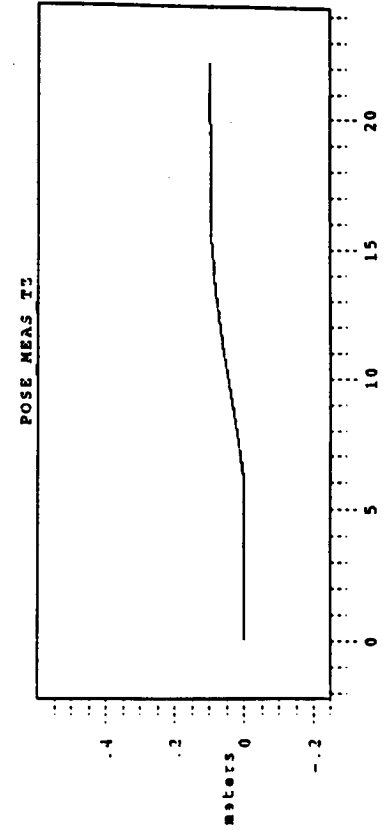
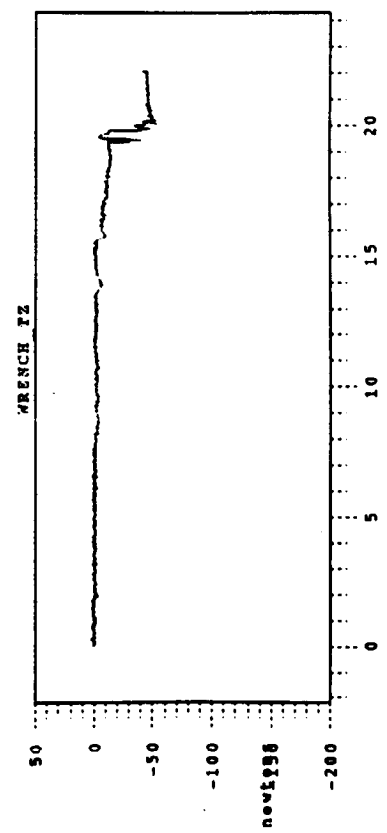
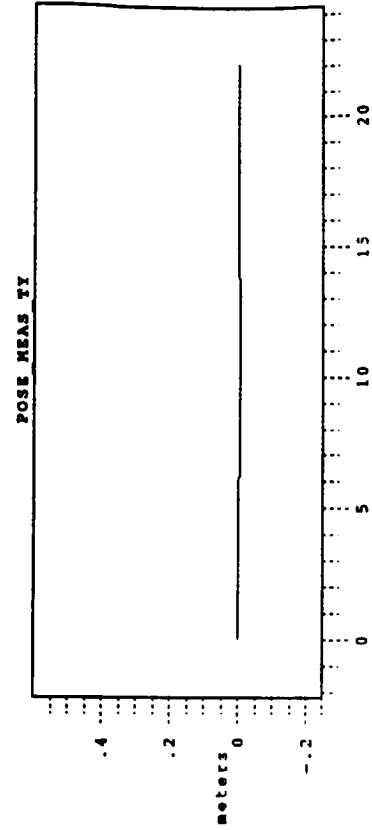
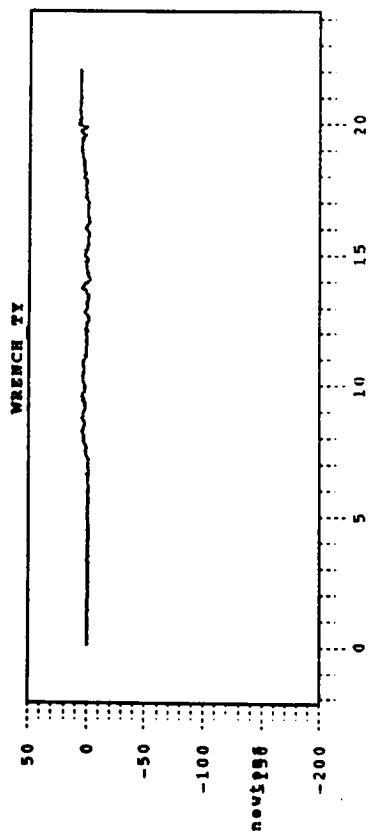
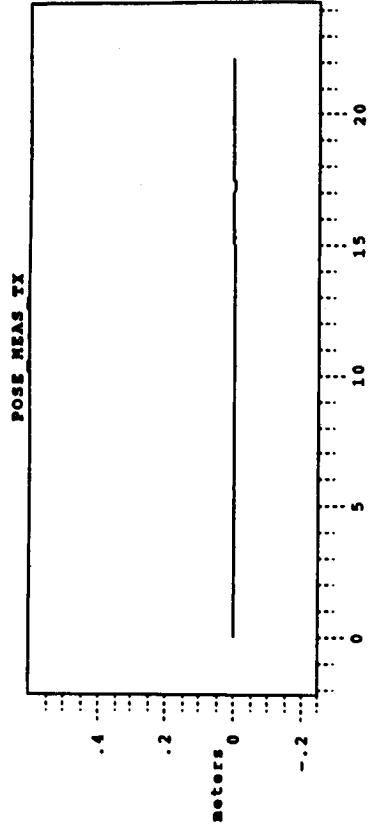
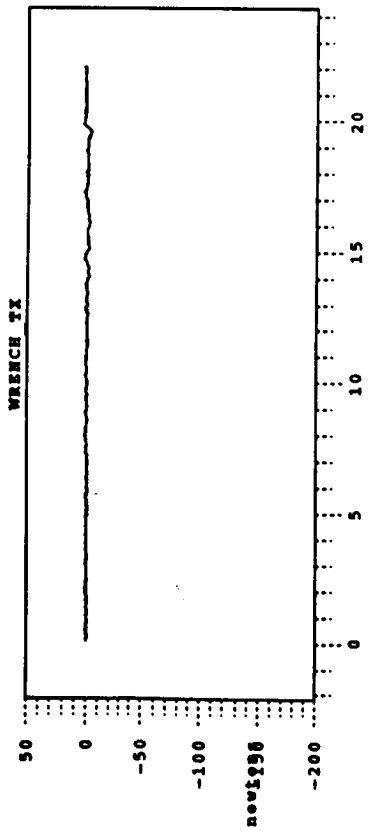
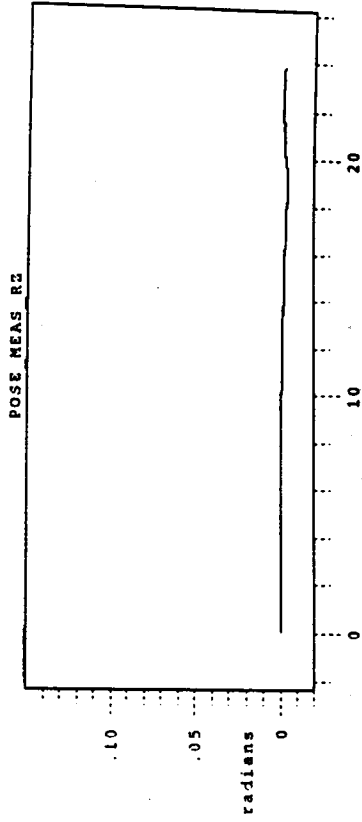
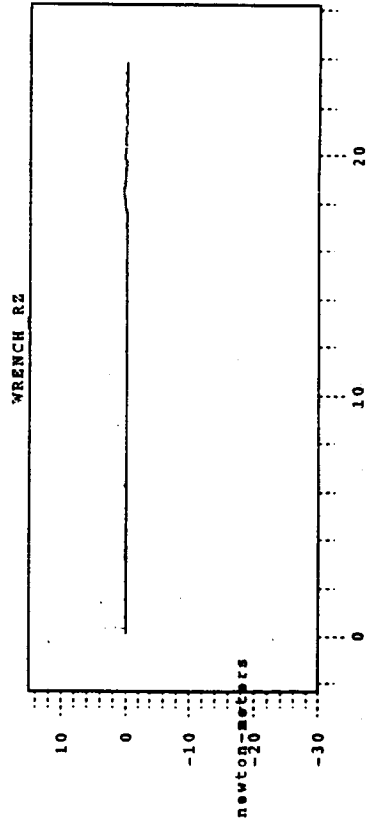
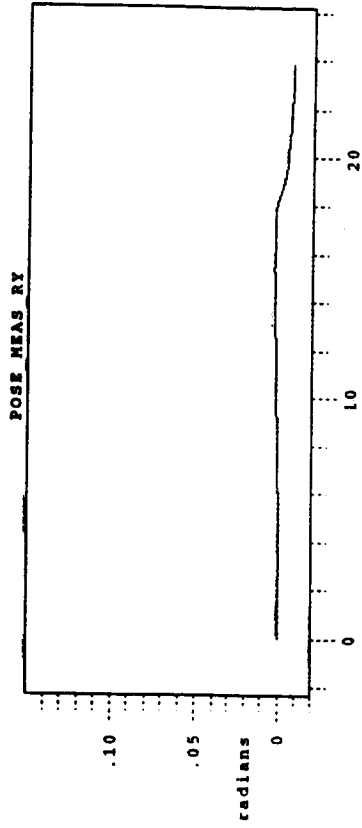
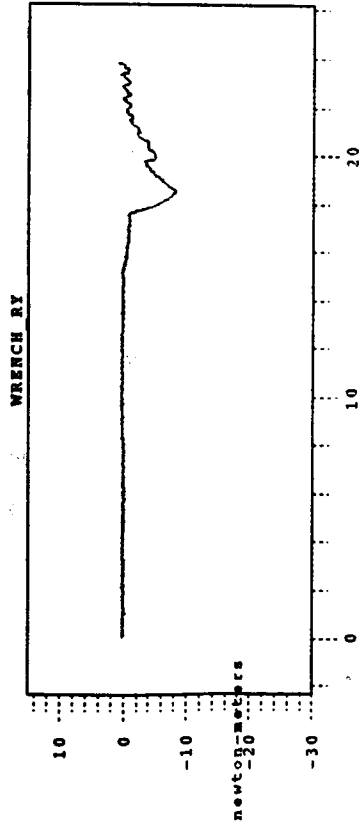
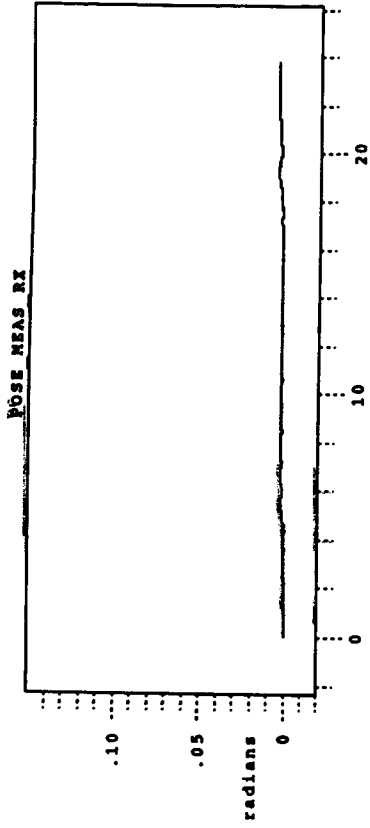
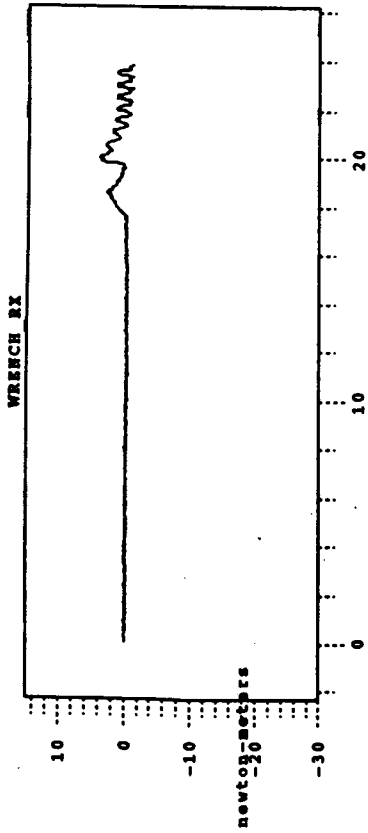


Figure 7



figures

File: (.LST)MATE_AUTO.PLOT

Time: 15:34:21.60 17-FEB-1993

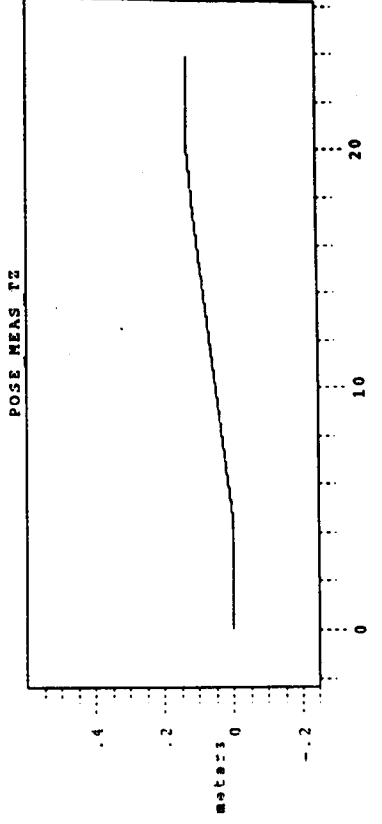
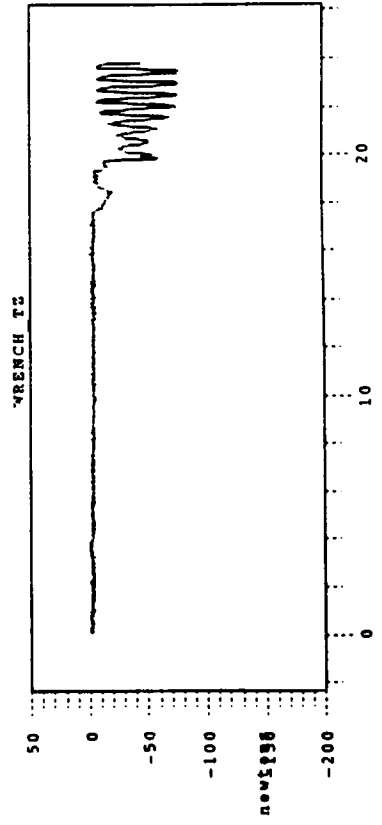
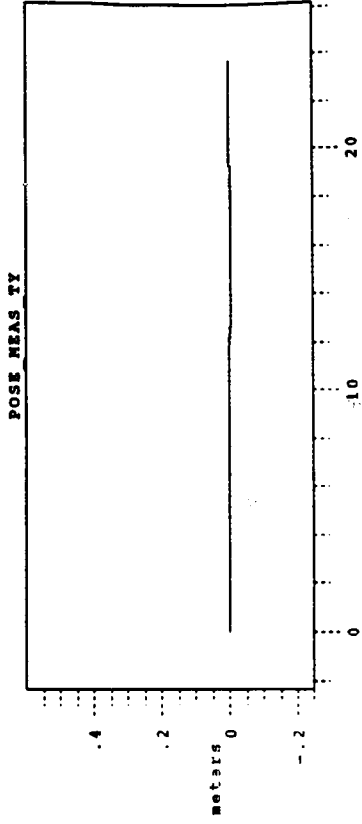
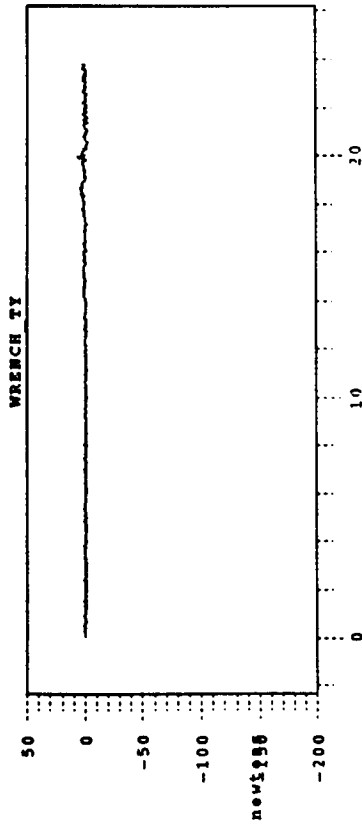
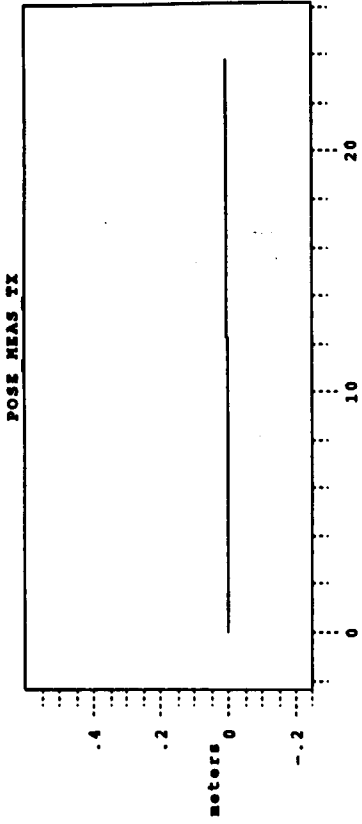
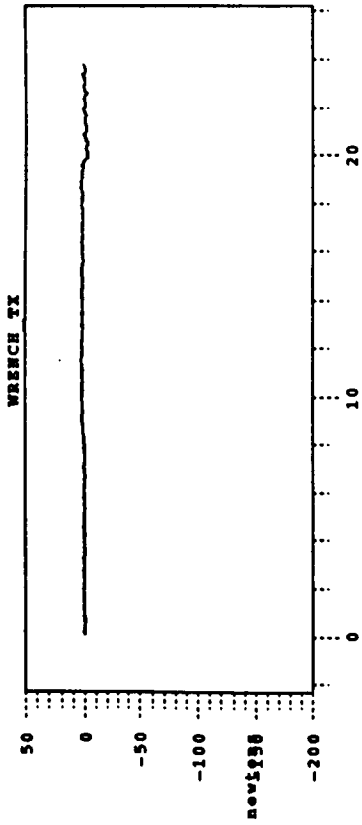


Figure 9

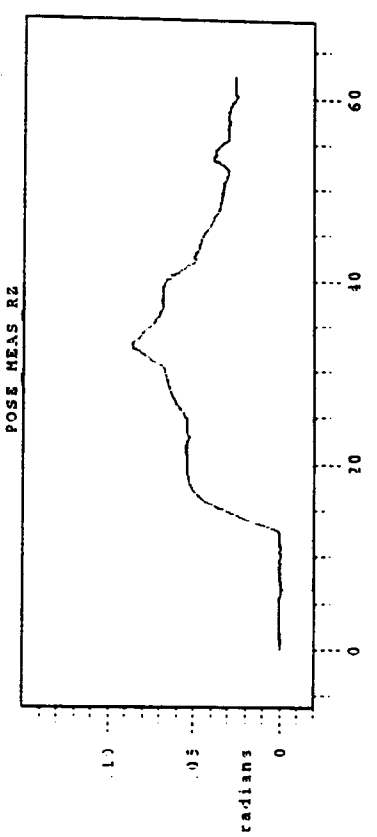
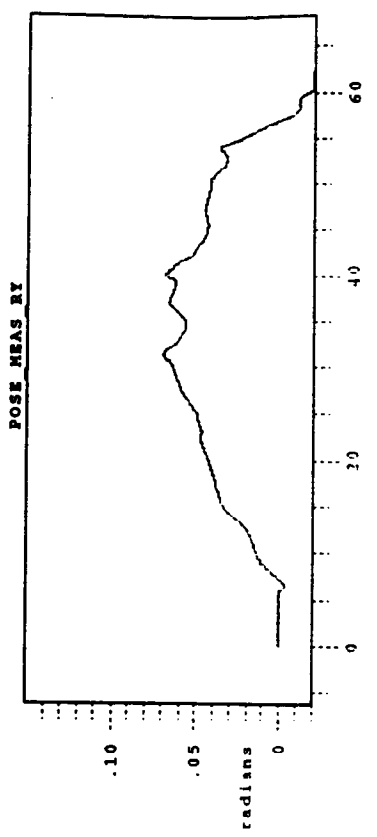
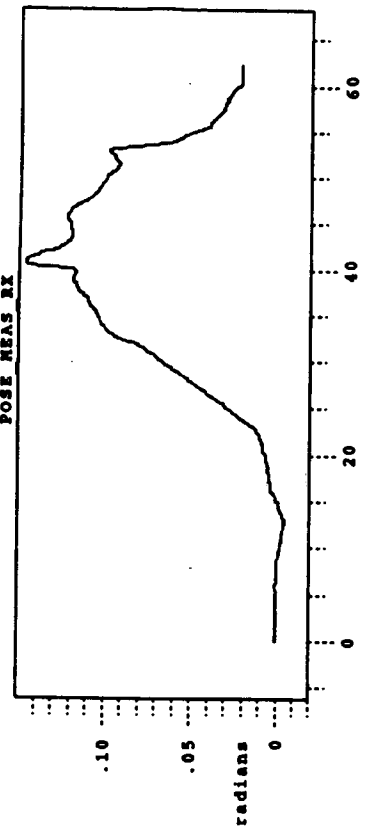
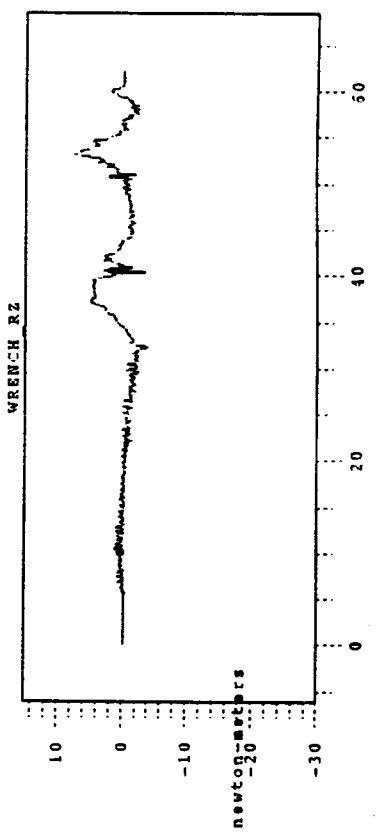
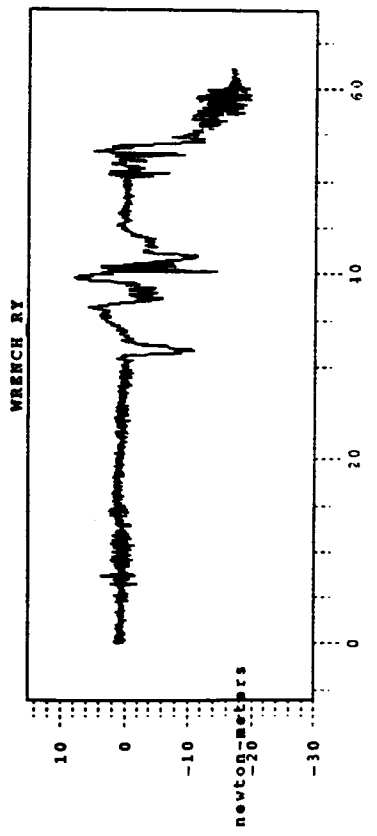
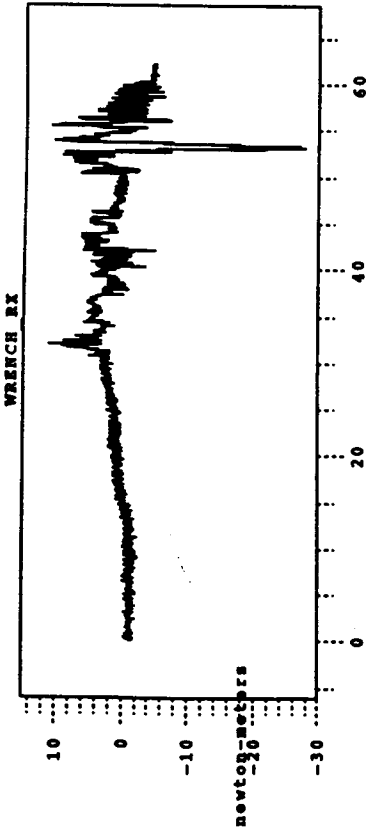


Figure 10

File: [..MNS]MATE_TELROP.PLOT

Time: 15:23:40.51 17-FEB-1993

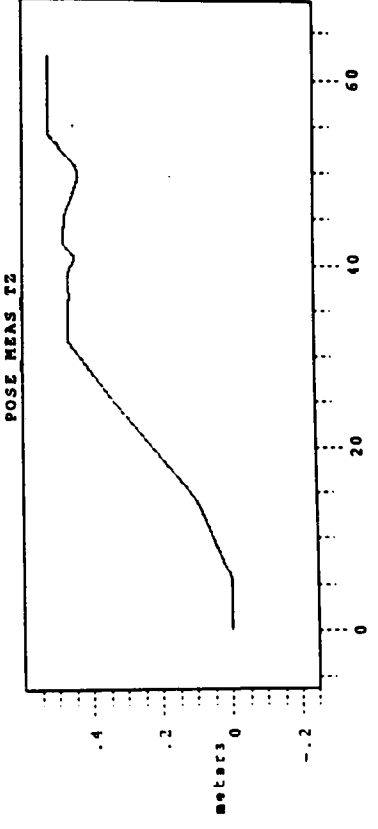
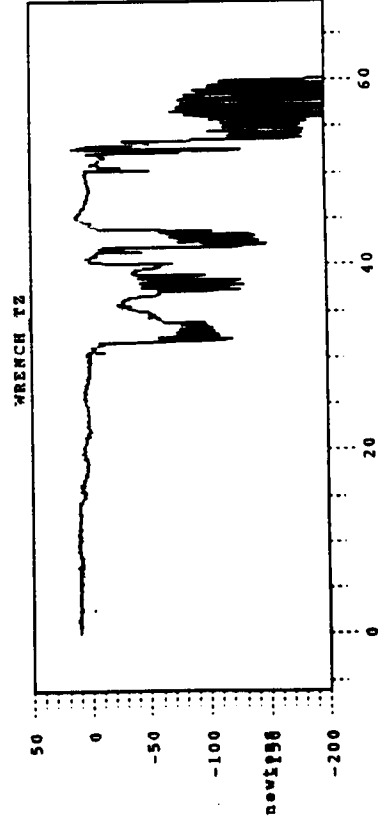
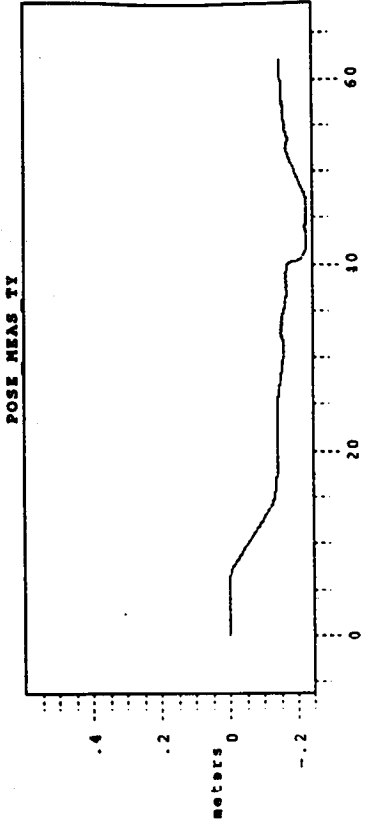
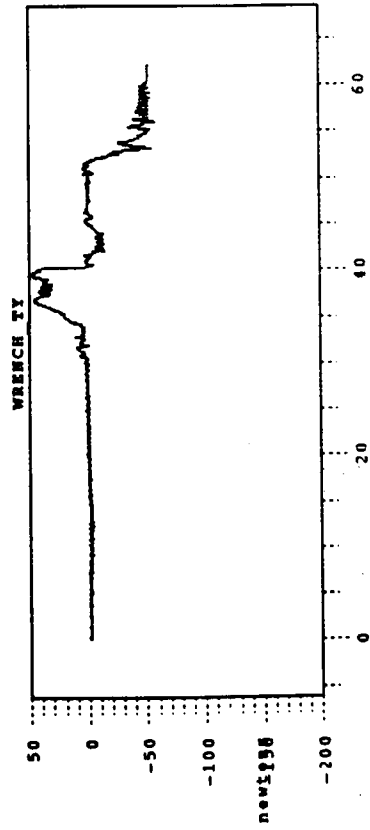
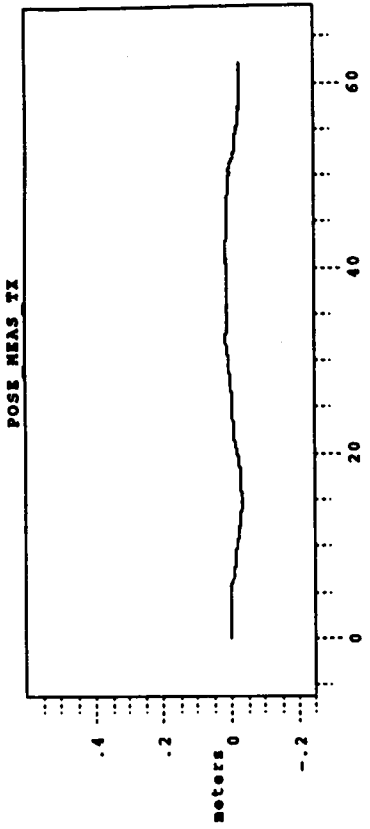
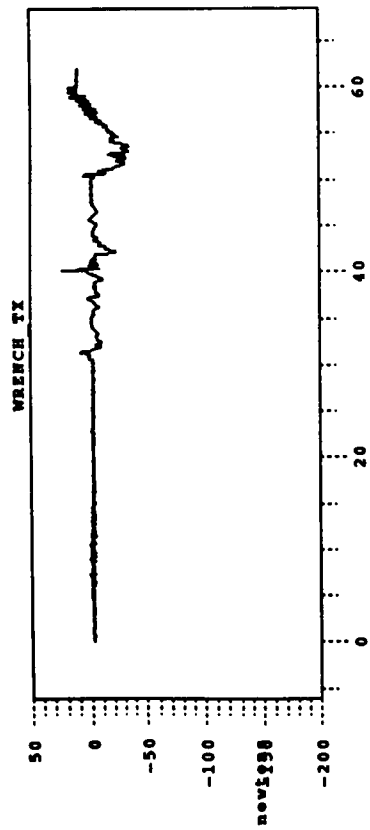


Figure 11

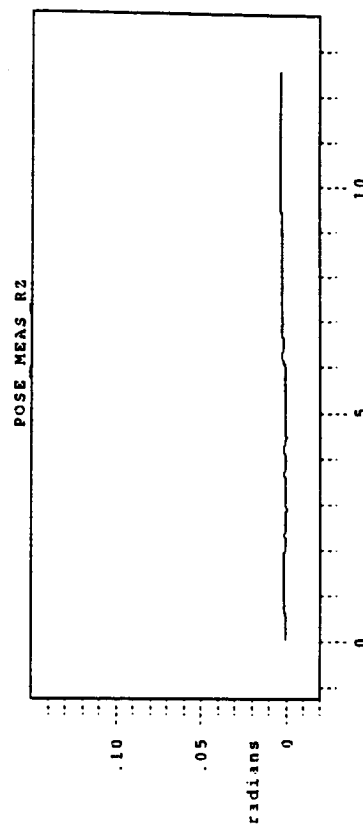
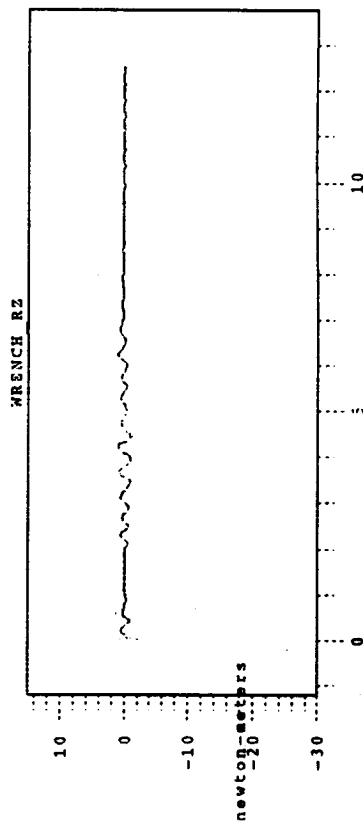
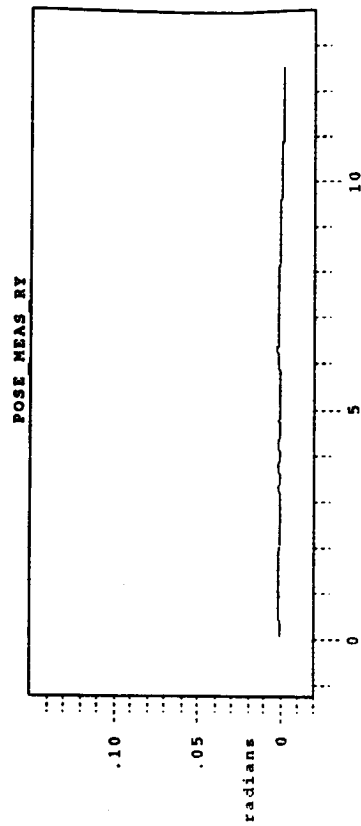
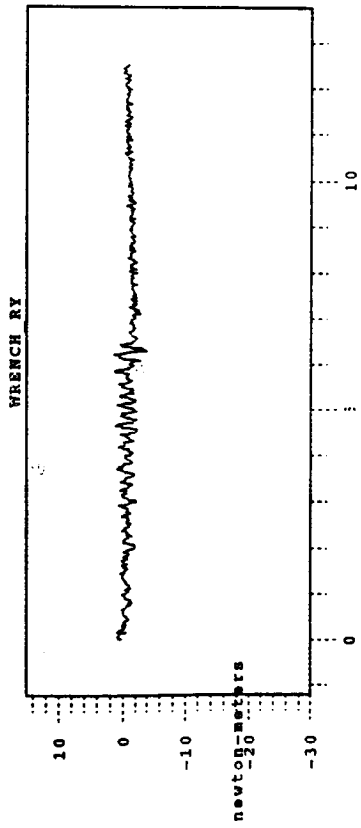
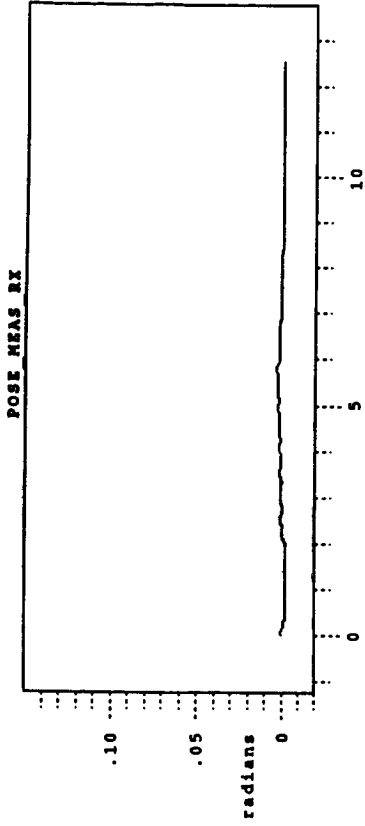
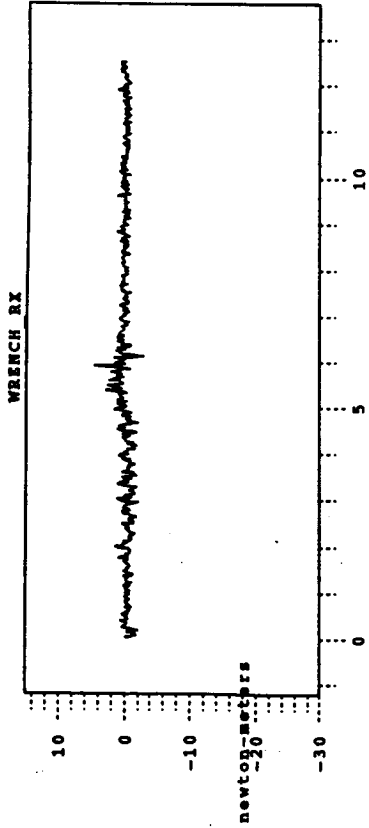


Figure 12

File: [.NMS]MATE_AUTO.PLOT

Time: 15:29:15.34 17-FEB-1993

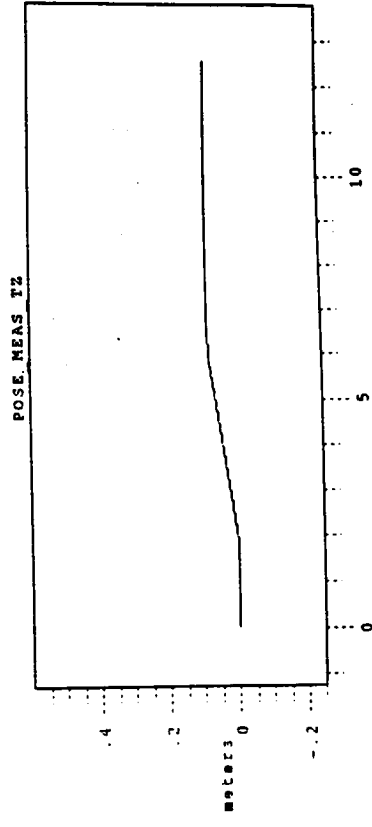
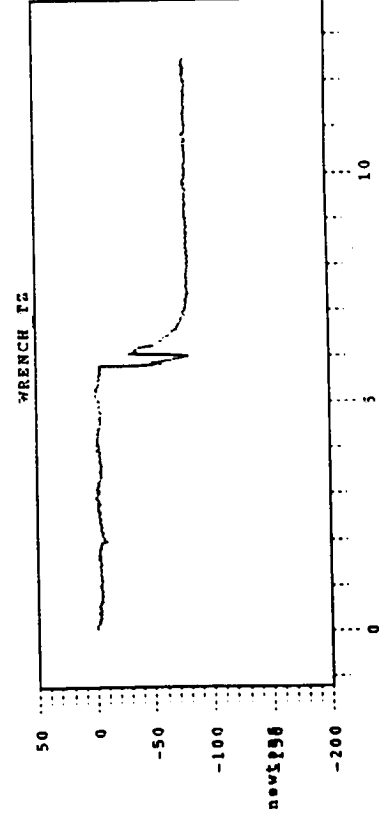
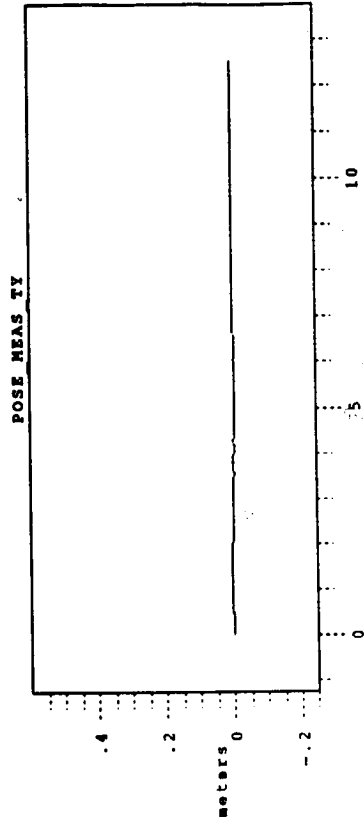
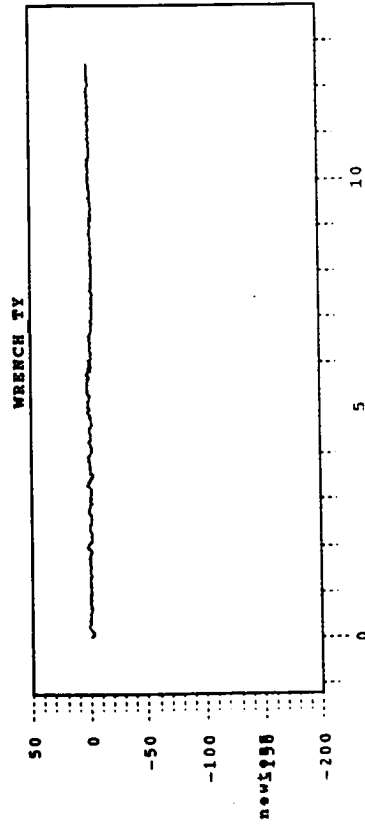
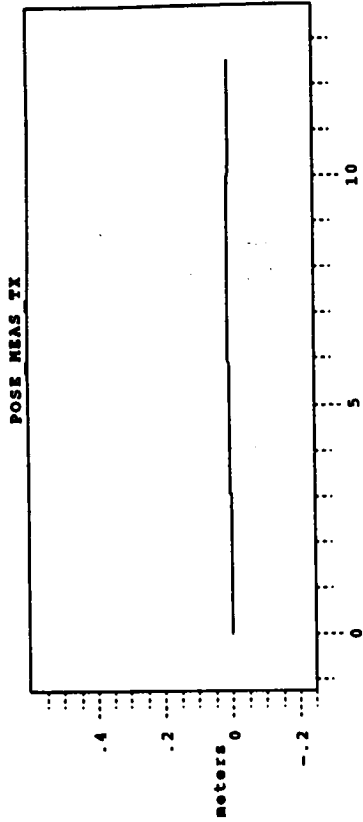
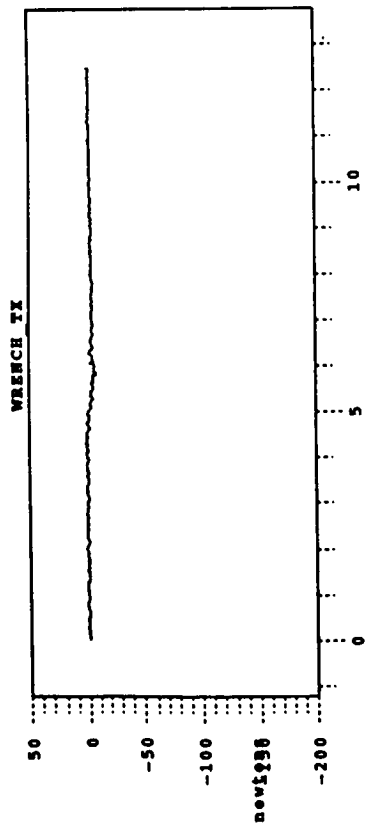


Figure 13